



ELSEVIER

Contents lists available at ScienceDirect

## Neoplasia

journal homepage: [www.elsevier.com/locate/neo](http://www.elsevier.com/locate/neo)

## PAX8 modulates the tumor microenvironment of high grade serous ovarian cancer through changes in the secretome



Amrita Salvi<sup>a</sup>, Laura R. Hardy<sup>a</sup>, Kimberly N. Heath<sup>a</sup>, Samantha Watry<sup>a</sup>, Melissa R. Pergande<sup>b</sup>,  
Stephanie M. Cologna<sup>b</sup>, Joanna E. Burdette<sup>a,\*</sup>

<sup>a</sup> Department of Pharmaceutical Sciences, College of Pharmacy, University of Illinois at Chicago, Chicago, IL 60607, USA

<sup>b</sup> Department of Chemistry, University of Illinois at Chicago, Chicago, IL 60607, USA

### ARTICLE INFO

#### Keywords:

Tumor microenvironment  
PAX8  
Fibronectin  
Tumor spheroids  
Ovarian cancer

### ABSTRACT

High grade serous ovarian cancer (HGSC) arises from the fimbriated end of the fallopian tube epithelium (FTE), and in some cases, the ovarian surface epithelium (OSE). PAX8 is a commonly used biomarker for HGSC and is expressed in ~90% of HGSC. Although the OSE does not express PAX8, murine models of HGSC derived from the OSE acquire PAX8, suggesting that it is not only a marker of Müllerian origin, but also an essential part of cancer progression, potentially from both the OSE and FTE. Previously, we have shown that PAX8 loss in HGSC cells causes tumor cell death and reduces cell migration and invasion. Herein, secretome analysis was performed in PAX8 deleted cells and we identified a reduction of the extracellular matrix (ECM) components, collagen and fibronectin. Immunoblotting and immunofluorescence in PAX8 deleted HGSC cells further validated the results from the secretome analysis. PAX8 loss reduced the amount of secreted TGFβ, a cytokine that plays a crucial role in remodelling the tumor microenvironment. Furthermore, PAX8 loss reduced the integrity of 3D spheroids and caused a reduction of ECM proteins fibronectin and collagen in 3D cultures. Due to the ubiquitous nature of PAX8 in HGSC, regardless of cell origin, and the association of its reduced expression with decreasing tumor burden, a PAX8 inhibitor could be a promising drug target against various types of HGSC. To accomplish this, we generated a murine oviductal epithelial (MOE) cell line stably expressing PAX8 promoter-luciferase. Using this cell line, we performed a screening assay with a library of FDA-approved drugs (Prestwick Library) and quantitatively assessed these compounds for their inhibition of PAX8. We identified two hits: losartan and captopril, both inhibitors of the renin-angiotensin pathway that inhibit PAX8 expression and function. Overall, this study validates PAX8 as a regulator of ECM deposition in the tumor microenvironment.

### Introduction

High grade serous ovarian cancer (HGSC) is the most common and lethal form of ovarian cancer with the lowest five-year survival rate. Current HGSC treatment involves surgical debulking followed by combination of platinum and taxane-based therapies. Despite the significant progress with respect to new therapies, most patients develop chemoresistance and succumb to the disease [1]. Immunotherapy in particular has shown limited success in epithelial ovarian cancer, mainly due to the challenges posed by the highly immunosuppressive HGSC tumor microenvironment (TME) [2]. The TME refers to the surrounding of the tumor cells, where tumor cells and immune cells can interact with the host stroma. The TME consists of a heterogeneous and interactive population of cancer cells and cancer stem cells along with the recruited stromal cells and endothelial cells. In addition to the cells, the TME comprises of

extracellular matrix (ECM) which includes proteins such as fibronectin, collagen, proteoglycans, and laminins as well as tumor-derived factors such as transforming growth factor beta (TGFβ), fibroblast growth factor (FGF), vascular endothelial growth factor (VEGF), matrix metalloproteases (MMPs) etc [2].

TGFβ is a cytokine secreted by tumor cells and fibroblasts and is involved in ECM remodeling leading to solid tumors [3]. Specifically, TGFβ mediates the transition of resident fibroblasts to cancer-associated fibroblasts (CAFs) to promote metastasis [4]. CAFs play a crucial role in ECM deposition and signaling interactions with cells of the TME [4]. ECM proteins such as fibronectin and collagen are both associated with disease aggressiveness by increasing tissue rigidity and enhancing infiltration of CAFs eventually impacting immune cell infiltration. Deposition of both collagen and fibronectin directly correlate with poor clinical prognosis and survival [5]. Fibronectin is an ECM glycoprotein that plays a crucial role in cell differentiation, migration, invasion, and proliferation in addition to processes such as wound healing, embryonic development and oncogenic transformation [6]. In ovarian cancer, fibronectin plays a role in cell migration, invasion, metastasis and acts as

\* Corresponding author.

E-mail address: [joannab@uic.edu](mailto:joannab@uic.edu) (J.E. Burdette).

**List of abbreviations**

$\alpha$ SMA	Alpha-smooth muscle actin
CAF	Cancer associated fibroblast
ChIP-Seq	Chromatin immunoprecipitation sequencing
COL1A1	Collagen 1
CRISPR	Clustered regularly interspaced short palindromic repeats
DAPI	4',6-diamidino-2-phenylindole
DMEM	Dulbecco's modified eagle media
DMSO	Dimethyl sulfoxide
DTT	Dithiothreitol
ECM	Extracellular matrix
EGF	Epidermal growth factor
EGTA	ethylene glycol-bis( $\beta$ -aminoethyl ether)-N,N,N',N'-tetraacetic acid
ELISA	Enzyme-linked immunosorbent assay
EMT	Epithelial to mesenchymal transition
FBS	Fetal bovine serum
FDA	Food and Drug administration
FDR	False discovery rate
FGF	Fibroblast growth factor
FOXM1	Forkhead box M1
FTE	Fallopian tube epithelium
GAPDH	Glyceraldehyde-3-phosphate dehydrogenase
GO	Gene Ontology
HGSC	High grade serous ovarian cancer
IHC	Immunohistochemistry
ITS	Insulin transferrin selenium
LC/MS	Liquid chromatography/mass spectrometry
MEM	Minimal essential media
MMP	Matric metalloprotease
MOE	Murine oviductal epithelium
mRNA	Messenger RNA
NOF	Normal ovarian fibroblast
OSE	Ovarian surface epithelium
P/S	Penicillin streptomycin
PARP	Poly ADP ribose polymerase
PAX8	Paired box transcription factor 8
PBS	Phosphate-buffered saline
PKC $\alpha$	Protein kinase C, alpha
qPCR	Quantitative polymerase chain reaction
RFP	Red fluorescent protein
RIPA	Radioimmunoprecipitation assay buffer
RLU	Relative luminescence units
RPMI	Roswell Park Memorial Institute medium
SDS	Sodium dodecyl sulfate
SILAC	Stable isotope labeling with amino acids in culture
shRNA	shRNA Small hairpin RNA
TGF $\beta$	Tumor growth factor, beta
TME	Tumor microenvironment
VEGF	Vascular endothelial growth factor

a prognostic biomarker [7–10]. Similar to fibronectin, collagen plays a role in ECM remodeling via controlling matrix stiffness and rigidity and provides a premetastatic niche in ovarian cancer cells [5,11].

Transcription factor Paired box 8 (PAX8) is involved in development of the fallopian tube epithelium (FTE) [12,13]. PAX8 is expressed in ~90% of HGSC and is a commonly used marker by pathologist to classify ovarian serous tumors [14]. The ovarian surface epithelium (OSE) typically does not express PAX8, however, murine models of HGSC derived from the OSE acquire PAX8, suggesting that it is not only a marker of Müllerian origin, but also essential for cancer progression, potentially from both the OSE and FTE [15]. PAX8 knockdown or deletion causes

reduction in tumor cell proliferation, migration and invasion [16–19]. More importantly, PAX8 loss reduces tumor burden in mice models of ovarian cancer [16]. Further, acquisition of PAX8 by OSE increases epithelial-mesenchymal transition (EMT) like morphology, migration, and invasion [19].

In this study, we found that PAX8 regulated the TME by enhancing fibronectin and collagen in HGSC cells and by increasing TGF $\beta$  secretion which increased alpha-smooth muscle actin ( $\alpha$ -SMA) expression in normal ovarian fibroblasts (NOFs). PAX8 loss reduced fibronectin expression in 3D tumor spheroids and reduced the integrity of spheroids. Additionally, we developed a PAX8 promoter-luciferase cell-based screening assay and identified losartan and captopril as novel repressors of PAX8 protein, which could reduce invasion by reducing PAX8 targets including FOXM1 and PKC $\alpha$  (PKCalpha) [16]. Altogether, this work increases our understanding of the role of PAX8 in modulating the HGSC secretome, which remodels the TME, and highlights the promising potential for novel PAX8 inhibitors.

**Materials and methods***Compounds*

Purchased compounds included thiostrepton (Cayman#19200), losartan potassium (Sigma#61188), sulfathiazole (Sigma#S9876), N-laurylsarcosine (Sigma#L7414), captopril (Sigma#C4042) atracurium besylate (Cayman#17796), L-DOPA (Cayman#13248), idoxuridine (Cayman#20222), dyphylline (Cayman#17958), dapsone (Cayman#23743), pyrimethamine (Cayman#16472), hydroflumethiazide (Cayman#23612), recombinant human TGF $\beta$ 1 (Peprotech#100-21), SB-431542 (Sigma#S4317). All compounds were suspended in dimethyl sulfoxide (DMSO), and final vehicle concentration was <0.1% (v/v).

*Cell culture*

Ovarian cancer cell lines (OVCAR-4 [RRID: CVCL\_1627], OVCAR-8 [RRID: CVCL\_1629]) and HEK293T (RRID: CVCL\_0063) cells were obtained from NCI Cell Bank. OVCAR8-RFP [OVCAR8 cells expressing red fluorescent protein (RFP)] were a gift from Sharon Stack at the University of Notre Dame (Indiana). OVCAR4 were grown in RPMI1640 supplemented with 2 mM L-glutamine, 10% fetal bovine serum (FBS, 100 I.U./mL), and 1% penicillin/streptomycin (P/S, 100 mg/mL). OVCAR8 cells, OVCAR8-RFP, and HEK293T were grown in DMEM with 10% FBS and 1% P/S. Ovarian fibroblast cell line (NOF) immortalized with p53 siRNA and hTERT called NOF151 (CVCL\_2G76) were a gift from Jinsong Liu [20]. These cells were maintained in Medium 199 and MCD105 medium (1:1) supplemented with 10% FBS, 1% P/S and 5  $\mu$ g Epidermal growth factor (EGF). Murine oviductal cells (MOE) were generated by Barbara Vanderhyden (Ottawa, CA) and cultured using  $\alpha$ -MEM-cellgro media (with ribonucleosides, deoxyribonucleosides and L-glutamine), supplemented with 10% FBS, 1% P/S, 1.8 ng/mL EGF, 2 mM L-glutamine, 1  $\mu$ g/mL gentamicin, 10  $\mu$ g/mL ITS, and 18.2 ng/mL  $\beta$ -estradiol. Cells were passaged a maximum of 20 times and maintained in a humidified incubator at 37 °C in a 5% CO<sub>2</sub> environment. All experiments were performed with mycoplasma free cells and all human cell lines have been authenticated using STR profiling <3 years.

*Plasmids and stable cell lines generation*

PAX8 shRNA was cloned in pLKO.1 plasmid (Millipore Sigma TRC Clone id TRCN0000021278). Lentiviral particles were generated by transfecting HEK293T cells with third-generation lentiviral packaging constructs pCMV-VSV-G (Addgene #8454) and pCMVR8.74 (Addgene #22036). Viral supernatant was used to transduce cells using polybrene followed by puromycin (1  $\mu$ g/mL) selection to generate single cell clones. For MOE cells expressing PAX8 promoter: cells were transfected with pGL4-PAX8 promoter-luciferase plasmid (Hygromycin) and

**Table 1**  
Primary antibodies.

Antibody	Source	Dilution for WB	Dilution for Immunofluorescence/ Immunohistochemistry
Anti-rabbit PARP	CST #9542	1:1000	-
Anti-rabbit GAPDH	CST #2118	1:10000	-
Anti-rabbit actin	Sigma #A2066	1:5000	-
Anti-rabbit PAX8	Proteintech #10336-1-AP	1:1000	1:50
Anti-rabbit PKC $\alpha$	CST #2056S	1:1000	-
Anti-rabbit COL1A1	Abcam #260043	1:500	1:50
Anti-rabbit fibronectin	Sigma #F3648	1:1000	1:50
Anti-mouse FOXM1	sc-376471	1:1000	-
Anti-mouse $\alpha$ -SMA	ab7817	1:1000	1:50
Alexa Fluor™ 594 Phalloidin	Invitrogen A12381	-	1:100

**Table 2**  
Secondary antibodies.

Antibody	Source	Dilution for WB	Dilution for immunofluorescence
Anti-rabbit IgG-HRP	CST #7074	1:10000	-
Anti-mouse IgG-HRP	CST #7076	1:10000	-
Anti-rabbit Alexa Fluor 488	Invitrogen# A-11034	-	1:1000

pLVX RFP Plasmid (Puromycin). Cells were selected with antibiotics Hygromycin (50  $\mu$ g/mL) and Puromycin (1 $\mu$ g/mL), followed by clonal selection. Clone verification was tested through luciferase assay.

#### SILAC sample preparation and data analysis

OVCAR8-RFP and OVCAR8-RFP PAX8<sup>-/-</sup> clone 2 were plated in T-25 flasks with SILAC DMEM Flex Media (Gibco) and cultured as described [21]. Cell pellets were lysed in RIPA buffer and 100 $\mu$ g of heavy and light were mixed at a 1:1 ratio for each biological replicate. Protein digestion was carried out using the FASP method followed by fractionation [22].

Raw data files were searched using Proteome Discoverer against the Human SwissProt database employing a decoy database, using standard settings with global FDR set at 1%. The mass tolerance for precursors was 10ppm and 0.02Da for the fragment ions. Trypsin was set as the protease, allowing two missed cleavages and fixed modification of carbamidomethyl (C) and variable modifications of <sup>13</sup>C<sub>6</sub><sup>15</sup>N<sub>4</sub> (R), <sup>13</sup>C<sub>6</sub><sup>15</sup>N<sub>2</sub> (K), oxidation (M) and deamidation (NQ). Only proteins with two unique peptides were used for quantitation. Proteomics data can be accessed online at: <ftp://massive.ucsd.edu/MSV000083585>.

#### Immunofluorescence analysis

Immunofluorescence was performed as described previously [23]. Actin was stained using phalloidin. Nuclei were stained with DAPI (0.1 mg/mL; Thermo Fisher Scientific #EN62248) for 10 min at room temperature. Images were acquired using 40X objective on a Nikon Eclipse E600 microscope using DS-Ri1 digital camera and NIS Elements Software (Nikon Instruments).

#### Immunoblot analysis

Cells/spheroids were lysed in RIPA buffer [50 mM Tris pH 7.6, 150 mM NaCl, 1% Triton X-100, 0.1% SDS with protease (Roche) and phosphatase (Sigma) inhibitors]. Immunoblot analysis was performed as described [23]. Membranes were incubated with primary antibody (Table 1) overnight at 4 °C. Membranes were incubated with secondary antibody (Table 2) prior to visualization of signal with SuperSignal™ West Femto substrate (Thermo Fisher) and imaging on a FluorChem E system (ProteinSimple).

#### Spheroids paraffin embedding

5,000 cells were resuspended in 100  $\mu$ L of media/well in 96-well round bottom Ultra Low Attachment Plate (Corning 07-201-680). After 14 days, the spheroids were collected, washed with 1X PBS and fixed with 4% paraformaldehyde for 4 h at room temperature. Spheroids were centrifuged, and paraformaldehyde was aspirated. Spheroid volume was estimated, suspended in equal volume of 2% agarose and mixed by pipetting. The tubes were placed at 4°C for 30 min and covered with 70% ethanol before paraffin embedding and sectioning.

#### Immunohistochemistry

Tumors/3D tumor spheroids were fixed with 4% paraformaldehyde followed by dehydration and paraffin embedding. Paraffin blocks were sectioned using standard histologic procedures. Hematoxylin and eosin staining (H & E) and immunohistochemistry were performed as described previously [24]. Sections were incubated with primary antibody (Table 1) followed by incubation with biotin or fluorophore-conjugated secondary antibody (Table 2). Sections were developed using 3,3'-diaminobenzidine to enable chromogenic detection. Tissues with secondary antibody treatment were used as a negative control. Masson's trichrome staining (Polysciences #25088) was performed as per kit manufacturer's instructions. Images were acquired on a Nikon Eclipse E600 microscope using a DS-Ri1 digital camera and NIS Elements Software (Nikon Instruments). Tumors used were from a previous animal study [16] performed in accordance with institution guidelines.

#### Matrigel invasion assay

1  $\times$  10<sup>5</sup> cells were added to a 0.8  $\mu$ M hanging insert (EMD Millipore Sigma, Burlington, MA) coated with 30  $\mu$ g/mL of matrigel (Fisher, Hampton, NH). After 24 h, non-invaded cells were washed away with PBS while invaded cells were stained with crystal violet (Sigma, St. Louis, MO) and quantified using ImageJ. Images were obtained using an AmScope MU900 with Touptview software (AmScope, Irvine, CA).

#### Spheroids viability assay

Spheroids were treated with compound/s and the plates were incubated at 37 °C. After 7 days, the plate was equilibrated to room temperature for 30 min and 100  $\mu$ L of CellTiter-Glo 3D Reagent (Promega) was added. The plate was incubated on a shaker for 30 min for complete

**Table 3**  
qRT-PCR primers.

Target gene	Forward primer sequence (5'-3')	Reverse primer sequence (5'-3')
<i>FN</i>	ACAACACCGAGGTGACTGAGAC	GGACACAACGATGCTTCCTGAG
<i>GAPDH</i>	ATGGGGAAGGTGAAGTTCG	GGGTCATTGATGGCAACAATA

lysis and luminescence was recorded using a Synergy Mx Plate Reader (BioTek).

#### Luciferase assay

MOE RFP-PAX8 promoter luciferase cells were plated in 24-well plates (60,000 cells per well) for 24 h to 80% confluency. Cells were treated with DMSO and Thio streptomycin as negative and positive controls at 2  $\mu$ M, respectively, and with the Prestwick library compounds at 1  $\mu$ M for 24 h. Cells were lysed after 24 h using lysis buffer (GME [Glycyl glycine, magnesium sulfate and EGTA] buffer, DTT, and TritonX), and frozen overnight at -80C. Subsequently, cells were thawed on a shaker to allow cell lysis and developed for RFP fluorescence levels using clear 96-well plates (Ex580, Em630). Further, luminescence was measured to determine whether the PAX8 promoter was repressed. Cell lysates were used immediately after developing for RFP to perform a luciferase assay using assay buffer (GME buffer, KPhos, ATP, and DTT) and luciferin (GME buffer, luciferin, and DTT). Following 24 h treatments with pure compounds, 110  $\mu$ L lysis buffer was added to each well and cells were frozen at -80C. Luciferase activity in relative luminescence units (RLU) was measured on a Synergy BioTek plate reader. Luciferase activity was normalized to RFP fluorescence.

#### cDNA synthesis and qRT-PCR analysis

Total RNA (1  $\mu$ g) was reverse transcribed to cDNA using iScript cDNA Synthesis Kit (Bio-Rad). qRT-PCR measurements were performed using the CFX connect Real-Time PCR Detection System (Bio-Rad) and SYBR Green (Roche) according to the manufacturer's protocol. Samples were normalized to the housekeeping gene, GAPDH. qRT-PCR primer sequences are provided in Table 3.

#### Live/dead imaging of spheroids

Live/dead staining of 3D tumor spheroids was performed using LIVE/DEAD™ Cell Imaging Kit (Invitrogen™ R37601) as per manufacturer's instructions. Images were acquired using 10X objective on a Nikon Eclipse E600 microscope using DS-Ri1 digital camera and NIS Elements Software (Nikon Instruments).

#### Statistical analysis

Data presented are the mean  $\pm$  standard error of the mean and represent at least 3 independent experiments. Statistical analysis was carried out using GraphPad Prism software. For the *in vitro* cell line experiments, two-sample t-tests were used for two groups. Adjusted  $p < 0.05$  is considered significant with stars denoting significance as follows: \* $p < 0.05$ , \*\* $p < 0.01$ , \*\*\* $p < 0.001$ , and \*\*\*\* $p < 0.0001$ .

## Results

### PAX8 enhanced secretion of multiple proteins that fall into the ECM pathway

Metastasis is a multi-step process which requires reprogramming of cells to acquire an oncogenic phenotype but also transformation of the tumor ECM to a pro-metastatic niche(1). PAX8 has a well-established role in cell migration, invasion and proliferation in ovarian cancer

[16,18,25–29]. Hence, we were interested in understanding if PAX8 plays a role in modulation of secreted proteins that impact the HGSC TME by investigating the secretome of HGSC cells with and without PAX8. To study this, we used OVCAR8-RFP cells, which are HGSC cells and knocked out PAX8 protein by the CRISPR-Cas9 method [16]. We performed SILAC (stable isotope labeling by amino acids in cell culture) of the secreted proteins in OVCAR8-RFP and OVCAR8-RFP PAX8<sup>-/-</sup> clones and analyzed the differentially expressed proteins by LC MS/MS (Fig. 1A). 749 proteins were found to be significantly differentially altered and KEGG pathway analysis of the top upregulated proteins identified ECM receptor interaction as the major pathway regulated by PAX8 in the secretome. Upon investigating the protein targets in these pathways, we found reduced expression of fibronectin, TGF $\beta$  and collagen 1 (COL1A1) in the secretome of PAX8 knockout cells (Fig. 1B). We performed ELISA to quantify the absolute concentrations of secreted TGF $\beta$  using conditioned media from OVCAR8-RFP and OVCAR8-RFP PAX8<sup>-/-</sup> cells. As shown in Fig. 1C, PAX8 loss reduced TGF $\beta$ 1 secretion. Similarly, expression of secreted fibronectin was significantly reduced using conditioned media from OVCAR8-RFP and OVCAR8-RFP PAX8<sup>-/-</sup> cells (Fig. 1D). Expression of fibronectin mRNA was significantly reduced in OVCAR8-RFP PAX8<sup>-/-</sup> cells relative to OVCAR8-RFP cells based on qPCR analysis (Fig. 1E).

### PAX8 enhanced downstream targets of TGF $\beta$

In order to validate the secretome data, we analyzed the expression of fibronectin and collagen using OVCAR4 and OVCAR8 cells with PAX8 expression reduced or knocked out. Generating PAX8 knockout OVCAR4 cells by the CRISPR method was lethal to the cells, hence we generated PAX8 knockdown cells using PAX8 specific shRNA. As shown in the immunofluorescence in Fig. 2A, loss of PAX8 reduced the fibronectin and collagen staining. We validated this finding by performing immunoblotting for fibronectin, which was reduced by PAX8 loss (Fig. 1B, Supplemental Fig. 1). Similarly, expression of collagen was found to be significantly reduced by loss of PAX8 in both OVCAR4 and OVCAR8 cells (Fig. 2A-B).

We have previously shown that mice injected with OVCAR8-RFP PAX8<sup>-/-</sup> have reduced tumor burden and better overall survival than mice injected with OVCAR8-RFP cells [16]. To determine if PAX8 regulated fibronectin and collagen expression *in vivo*, we performed immunohistochemistry for PAX8, fibronectin and collagen expression in these tumors. As shown in Fig. 2C, we found that loss of PAX8 reduced fibronectin and collagen staining in the tumor sections (indicated by arrows). To assess the degree of fibrosis in the tumors, we performed Masson's trichrome staining of collagen and found that PAX8 loss reduced total collagen expression in the tumor sections (Fig. 2C).

### Loss of PAX8 reduced fibronectin expression in tumor spheroids

Since our *in vitro* data strongly suggested PAX8 regulated expression of ECM proteins fibronectin and COL1A1, we generated 3D tumor spheroids using OVCAR8-RFP and PAX8 knockout cells by growing the cells in ultra-low adhesion plates. In comparison with 2D cell culture models, 3D spheroids are able to accurately mimic some features of solid tumors, such as their spatial architecture, physiological responses, gene expression patterns and drug resistance mechanisms [30]. As shown in Fig. 3A, we found that although PAX8 knockout spheroids were larger in size (as shown in the brightfield images), they were not as bright based on RFP in the fluorescent images.

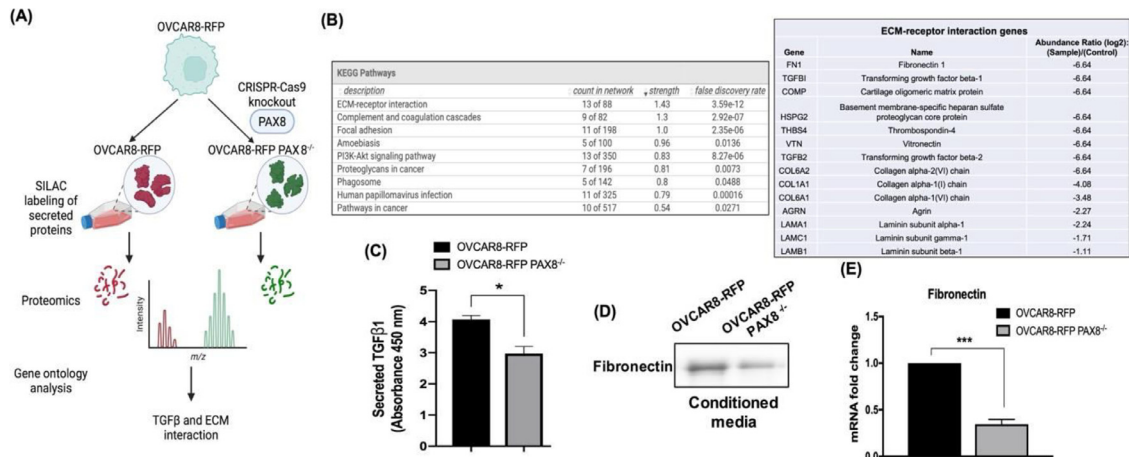


**Fig. 1. PAX8 enhanced secretion of multiple proteins involved in Extracellular Matrix (ECM) remodeling.** A. Workflow of SILAC labeling. B. String database was used to perform a KEGG pathway analysis on the differentially altered proteins. Nine pathways were identified of which top 3 pathways (Left table) were significant with a strength  $\geq 1$  and a false discovery rate  $< 2.5e-06$ . Right table represents list of genes in the ECM-receptor interaction pathway with abundance ratio of (OVCAR8-RFP PAX8<sup>-/-</sup>)/(OVCAR8-RFP). C. TGFβ1 concentration from conditioned media of OVCAR8-RFP and OVCAR8-RFP PAX8<sup>-/-</sup> cells assayed by ELISA. D. Representative immunoblot for fibronectin expression in conditioned media of OVCAR8-RFP and OVCAR8-RFP PAX8<sup>-/-</sup> cells. E. Validation of fibronectin expression by qPCR in OVCAR8-RFP and OVCAR8-RFP PAX8<sup>-/-</sup> cells.

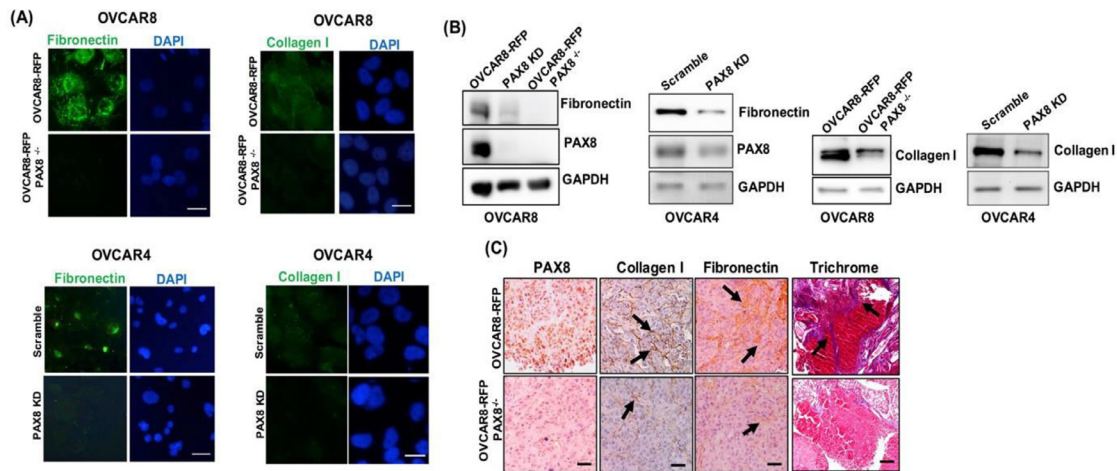


**Fig. 2. PAX8 enhanced downstream targets of TGFβ1.** A. Representative immunofluorescence images for fibronectin and collagen 1 expression in OVCAR4 and OVCAR8 cells with knockout or knockdown of PAX8. DAPI was used as a nuclear stain. Scale bar = 20 μm. B. Representative immunoblot for fibronectin, collagen 1 and PAX8 expression in OVCAR4 and OVCAR8 cells with knockout and knockdown of PAX8. GAPDH was used as a loading control. C. Representative immunohistochemistry images for PAX8, fibronectin and collagen 1 expression in tumor sections from OVCAR8-RFP and OVCAR8-RFP PAX8<sup>-/-</sup> xenografts. Masson's Trichrome staining using tumor sections from OVCAR8-RFP and OVCAR8-RFP PAX8<sup>-/-</sup> xenografts. Scale bar = 50 μm.

We performed immunohistochemistry on the spheroids and found that loss of PAX8 reduced fibronectin expression (Fig. 3B). This finding was consistent with immunofluorescence staining (Fig. 3C). Additionally, immunoblotting of the spheroids demonstrated reduced expression of fibronectin consistent with the 2D culture data (Fig. 3D). PAX8 knock-out spheroids also showed reduced expression of COL1A1 and PAX8 downstream effectors such as FOXM1 and PKCα (Fig. 3D).

*PAX8 regulated TGFβ secretion drives CAF transformation*

TGFβ is a cytokine secreted by tumor cells and fibroblasts, which alters the ECM leading to tumor rigidity [3]. Specifically, TGFβ mediates the transition of resident fibroblasts to CAFs and promotes cancer metastasis [4]. Since we found that PAX8 regulated secretion of TGFβ1 (Fig. 1C), we were interested in determining if this was sufficient to block fibroblasts acquisition of CAF markers. We used conditioned media from OVCAR8 cells and OVCAR8-PAX8 knockout cells and added it to ovarian fibroblast cells, NOF151. TGFβ (exogenous) was used as

positive control and we determined expression of alpha-smooth muscle actin (α-SMA), which is a marker of CAFs. As shown in the immunoblot in Fig. 4A-B, conditioned media from OVCAR8 and OVCAR4 cells was able to induce expression of α-SMA after 3 days whereas media from PAX8 knockout cells did not induce α-SMA expression. We used a TGFβ inhibitor (SB-431542) to confirm if the induction of α-SMA was caused by TGFβ and we found this effect abolished by using the TGFβ inhibitor (Fig. 4A-B). We also investigated expression of α-SMA in PAX8 expressing and knockout tumor xenografts by immunohistochemistry and found reduced expression of α-SMA in PAX8 knockout animals (Fig. 4C).

*Identification of PAX8 inhibitors as novel therapeutics in HGSC*

Loss of PAX8 in normal FTE did not demonstrate any significant alterations in cell survival or morphology, whereas in HGSC cells, PAX8 loss caused reduced cell invasion, migration and tumor burden [16,19]. Hence, reducing PAX8 levels as a therapeutic strategy would leave normal cells unaffected, while decreasing HGSC progression. Previously,

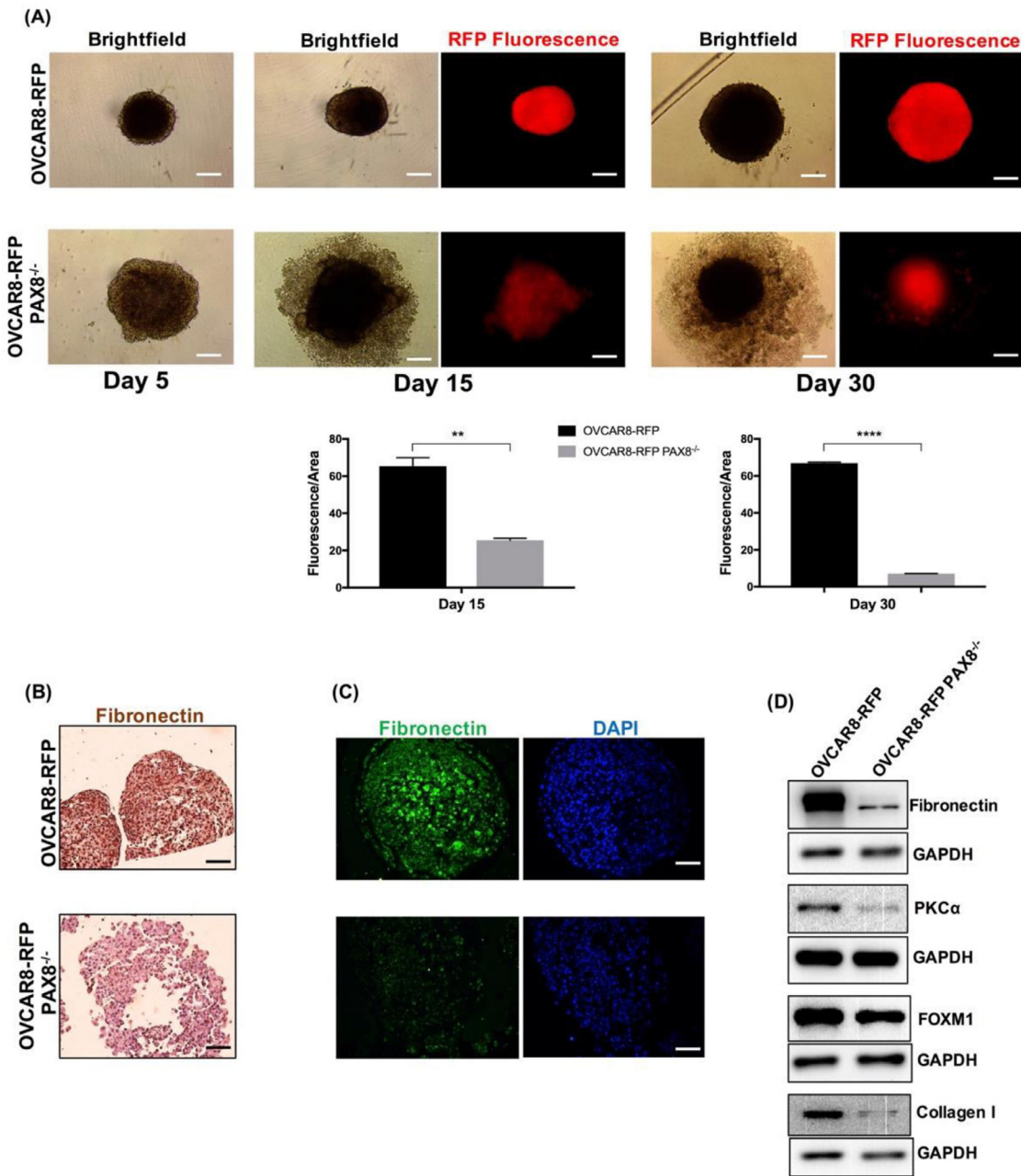


**Fig. 3. Loss of PAX8 reduced fibronectin expression in tumor spheroids.** A. Representative brightfield and RFP fluorescence images of 3D tumor spheroids generated from OVCAR8-RFP and OVCAR8-RFP PAX8<sup>-/-</sup> cells capture at Day 5, 15 and 30. Scale bar = 500 μm. Graph represents quantification of (Red fluorescence intensity/Area) of the spheroids using ImageJ software. B. Representative immunohistochemistry images for fibronectin expression in 3D tumor spheroids generated from OVCAR8-RFP and OVCAR8-RFP PAX8<sup>-/-</sup> cells. Scale bar = 500 μm. C. Representative immunofluorescence images for fibronectin expression in 3D tumor spheroids generated from OVCAR8-RFP and OVCAR8-RFP PAX8<sup>-/-</sup> cells. DAPI was used as a nuclear stain. Scale bar = 500 μm. D. Representative immunoblot for fibronectin, PKCα, FOXM1 and Collagen I expression in expression in 3D tumor spheroids generated from OVCAR8-RFP and OVCAR8-RFP PAX8<sup>-/-</sup> cells. GAPDH was used as a loading control.

we identified thioestrepton as a small molecule that decreases PAX8 protein levels, however thioestrepton is not a viable drug lead due to poor solubility [16]. Therefore, to identify novel PAX8 inhibitors, we developed a high-throughput screening (HTS) assay by generating a stable murine oviductal epithelial (MOE) cell line expressing the PAX8 promoter tagged with luciferase. This cell line expresses a stable red fluorescent protein (RFP) driven by a CMV promoter as an internal control to counter screen for reduced cell viability (Fig. 5A). Nontumorigenic MOE cells were used because these are resistant to growth inhibition from loss of PAX8, whereas cancer cell lines would be predicted to undergo cell death from PAX8 loss [19,27,28,31,32]. Importantly, the

PAX8 promoter has multiple PAX8 binding sites, thus the reporter cell line can detect small molecules that either block transcription or those that downregulate PAX8 protein abundance [33].

Using thioestrepton as a positive control, the Z' factor for the assay is 0.6, which is an acceptable value for HTS. We screened the Prestwick library of compounds (which is a library of 1,200 FDA approved compounds) and identified 15 compounds which could repress PAX8 promoter activity (Fig. 5B). Interestingly, a recent study found that losartan reduces fibronectin and collagen levels in ovarian cancer cells [34,35]. Both losartan and captopril are inhibitors of the renin-angiotensin signaling pathway and because we found captopril in our screen, we in-

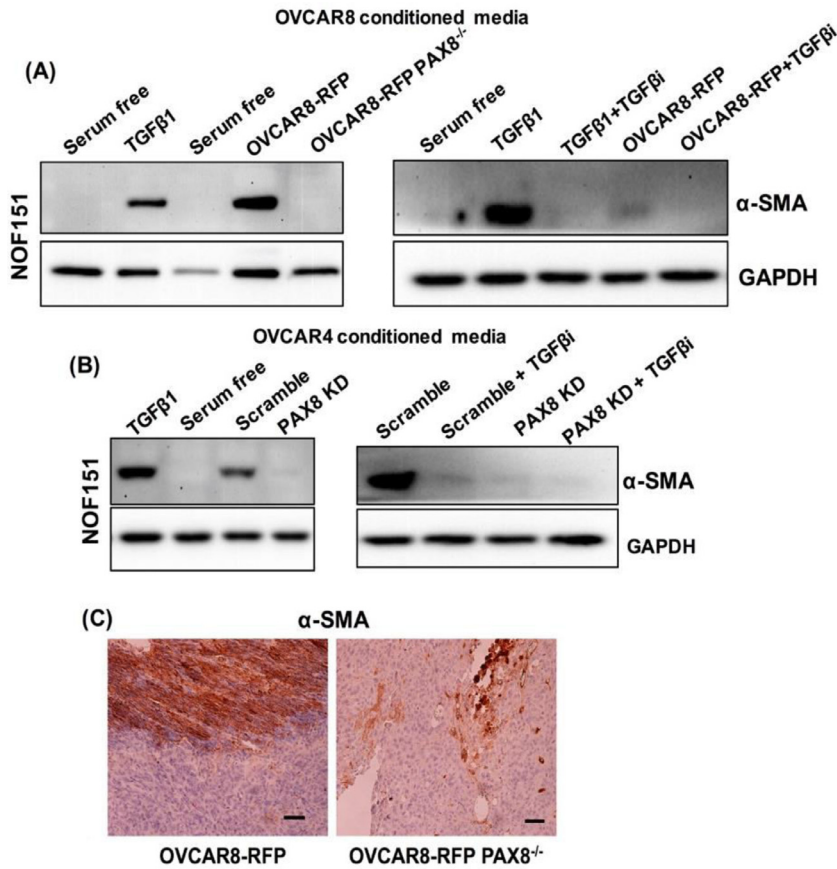


**Fig. 4.** PAX8 regulated TGF $\beta$  secretion drives CAF transformation in NOF151 cells. A. NOF151 cells were treated with conditioned serum-free media from OVCAR8-RFP and OVCAR8-RFP PAX8<sup>-/-</sup> cells for 3 days. TGF $\beta$ 1 (10 ng/ml) was used as positive control. SB-431542 (10 $\mu$ M) was used as a TGF $\beta$  inhibitor (TGF $\beta$ i). Immunoblot analysis was performed for  $\alpha$ -SMA (Alpha-Smooth muscle actin) in NOF151 cells. GAPDH was used as a loading control. B. NOF151 cells were treated with conditioned serum-free media from OVCAR4 and OVCAR4-PAX8 KD cells for 3 days. TGF $\beta$ 1 (10 ng/ml) was used as positive control. SB-431542 (10 $\mu$ M) was used as a TGF $\beta$  inhibitor (TGF $\beta$ i). Immunoblot analysis was performed for  $\alpha$ -SMA in NOF151 cells. GAPDH was used as a loading control. C. Representative immunohistochemistry for  $\alpha$ -SMA expression of tumor sections from OVCAR8-RFP and OVCAR8-RFP PAX8<sup>-/-</sup> xenografts. Scale bar = 50  $\mu$ m.

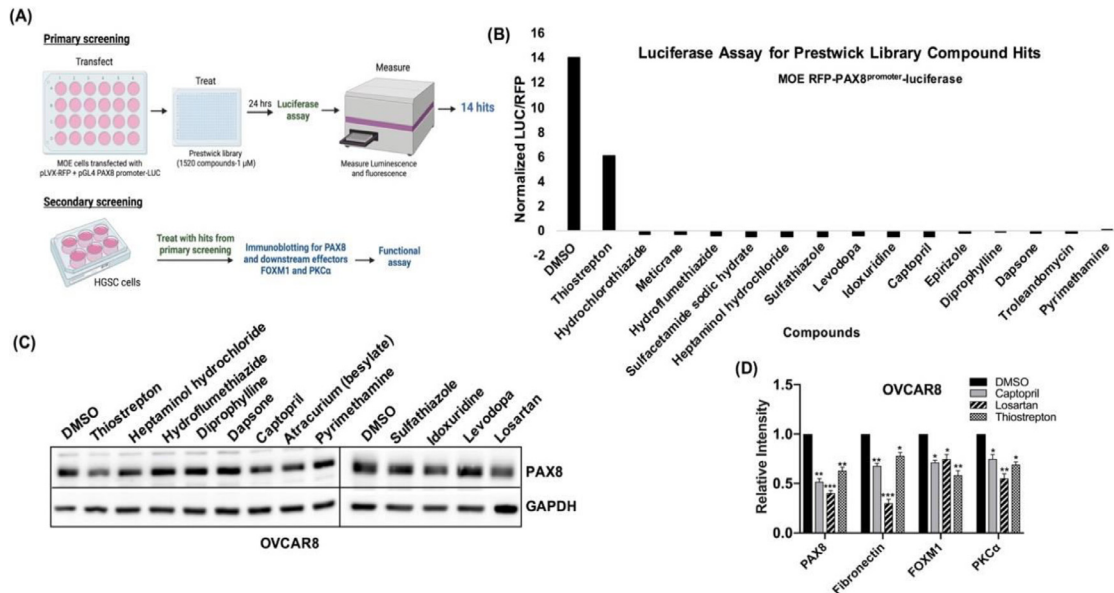


**Fig. 5.** PAX8 inhibitors: losartan and captopril reduced PAX8 and fibronectin expression in tumor spheroids. A. Workflow for Prestwick library screening using MOE RFP-PAX8<sup>promoter</sup>-luciferase cell line. B. Luciferase assay results of MOE-PAX8 promoter-LUC cells treated with 1 $\mu$ M of compounds from the Prestwick library. Graph indicates normalized luciferase/RFP fluorescence values for 15 hits identified from luciferase assay. C. Representative immunoblot for PAX8 expression in OVCAR8 cells treated with vehicle control (DMSO) and hit compounds from Prestwick library screening. GAPDH was used as a loading control. D. Densitometry analysis for PAX8, fibronectin, FOXM1 and PKC $\alpha$  expression for OVCAR8 cells treated with vehicle control (DMSO), losartan (1 $\mu$ M), captopril (1 $\mu$ M) and thioestron (1 $\mu$ M). Normalization was performed relative to loading control GAPDH.

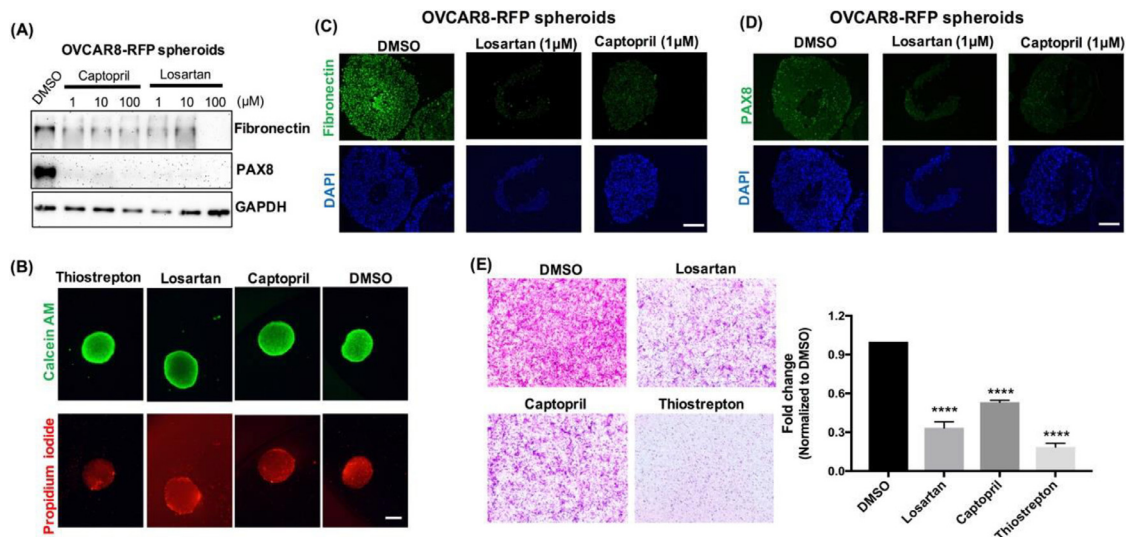


**Fig. 6. PAX8 inhibitors: losartan and captopril reduced PAX8 and fibronectin expression in tumor spheroids and reduced cell invasion.** A. Representative immunoblot for fibronectin and PAX8 expression in 3D tumor spheroids generated from OVCAR8-RFP cells and treated with vehicle control (DMSO), losartan and captopril. GAPDH was used as a loading control. B. Representative fluorescence images for Live/Dead imaging performed in 3D tumor spheroids generated from OVCAR8 cells and treated with vehicle control (DMSO), losartan captopril and thiostrepton. Scale bar = 500  $\mu$ m. C. Representative immunofluorescence images for fibronectin expression in 3D tumor spheroids generated from OVCAR8-RFP cells and treated with vehicle control (DMSO), losartan and captopril. DAPI was used as a nuclear stain. Scale bar = 500  $\mu$ m. D. Representative immunofluorescence images for PAX8 expression in 3D tumor spheroids generated from OVCAR8-RFP cells and treated with vehicle control (DMSO), losartan and captopril. DAPI was used as a nuclear stain. Scale bar = 500  $\mu$ m. E. Representative images for Boyden chamber invasion assay using matrigel. OVCAR8 cells were treated with vehicle control (DMSO), losartan, captopril and thiostrepton for 24 h. Invaded cells are stained with crystal violet and quantified using microscopy.

investigated and confirmed that losartan reduced PAX8 protein levels and fibronectin expression in HGSC cells [36,37]. We performed a secondary screening assay by immunoblotting for PAX8 and identified losartan and captopril as compounds that consistently reduced PAX8 promoter activity and protein expression (Fig. 5C-D, Supplemental Fig. 2). Previously, we reported that PAX8 played a role in tumor cell migration and invasion by regulating expression of FOXM1 and PKC $\alpha$  [16]. As shown in Fig. 5D, both losartan and captopril reduced expression of PAX8, fibronectin, and PAX8 downstream proteins such as FOXM1 and PKC $\alpha$  in OVCAR8 cells.

#### *PAX8 inhibitors: losartan and captopril reduced PAX8 and fibronectin expression in tumor spheroids*

Losartan and captopril were interesting therapeutic leads because in the context of cancer captopril was shown to inhibit tumor angiogenesis and losartan was shown to improve response to chemotherapy in ovarian cancer [34,37]. PAX8 has a well-established role in cancer cell invasion [16,19,27,38]. To investigate whether losartan and captopril reduce viability and PAX8 expression in 3D tumor spheroids, we generated tumor spheroids using OVCAR8 cells and treated them with losartan and captopril. We performed immunoblotting analysis of the spheroids and found that both losartan and captopril were able to reduce expression of fibronectin and PAX8 compared to vehicle control DMSO (Fig. 6A). There was no change in viability of the spheroids as shown by live/dead imaging by captopril treatment. Losartan and thiostrepton treatment reduced spheroid viability as shown by reduced Calcein AM staining, spheroid viability assay and immunoblotting for apoptosis marker cleaved poly ADP ribose polymerase (PARP) (Fig. 6B, Supplemental Fig. 3). Immunofluorescence staining on spheroids showed that treatment of spheroids with losartan and captopril reduced fibronectin and PAX8 expression (Fig. 6C-D). In order to determine if these compounds affect PAX8-mediated cell invasion, we performed a Matrigel invasion assay. Losartan, captopril and thiostrepton significantly decreased the invasive ability of OVCAR8 cells relative to the vehicle control (Fig. 6E).

#### Discussion

PAX8 has a well-established pro-tumorigenic role in high grade serous cancer cells and in altering the genome as a transcription factor [18,26–29,31,32,38,39]. However, little has been studied regarding the proteome and particularly the secreted proteins that are altered by PAX8 expression. This is the first study to connect PAX8 as a regulator of ECM deposition in the TME of HGSC. Herein, we demonstrate that PAX8 regulated expression of ECM proteins: TGF $\beta$ , fibronectin and collagen. Furthermore, using a PAX8 promoter-based screening assay, we identified losartan and captopril as novel FDA approved compounds that function to repress PAX8 expression and PAX8 downstream targets, such as FOXM1 and PKC $\alpha$ .

Mass spectrometry-based proteomics of the secretome of the PAX8 expressing HGSC cells compared to PAX8<sup>-/-</sup> cells revealed TGF $\beta$  and ECM receptor interactions as major pathways impacted. The ECM protein alterations that were significantly changed include, collagen 1 and fibronectin, which are both associated with more aggressive disease by increasing tissue rigidity, enhancing infiltration of CAFs, and hampering immune cell infiltration [40]. Our *in vitro* and *in vivo* data showed that PAX8 loss caused a significant reduction in fibronectin mRNA and protein expression. This finding was supported in a recent study by Bleu et al., where the authors using the BioID system identified PAX8 and MECOM (MDS1 and EVI1 complex locus) to form a transcriptional complex which was found to regulate gene expression module involved in focal adhesion, TGF $\beta$  signaling and ECM. Fibronectin was identified as one of top genes regulated by the PAX8-MECOM complex driving ovarian cancer [29]. Previously, our lab and others have shown using RNA-Seq analysis that loss of PAX8 in HGSC cells causes a significant change in transcripts associated with ECM and cytoskeletal rearrangements [16,25,28,31]. Further, silencing PAX8 was shown to reduce the ability of ovarian cancer cells to migrate and adhere to ECM substrate specifically collagen and fibronectin [25]. Conditioned media from PAX8 expressing HGSC cells caused the transition of normal ovarian fibroblasts to form CAFs and a TGF $\beta$  inhibitor attenuated this effect. Conditioned media from PAX8 knockout cells blocked this transi-

tion possibly due to reduced expression of secreted TGF $\beta$  caused by loss of PAX8. These data strongly suggest that in addition to regulating fibronectin expression in HGSC cells, PAX8 mediated TGF $\beta$  secretion also impacts surrounding stroma in the TME.

Since PAX8 is a transcription factor, a number of studies have evaluated PAX8 gene targets by RNA-Seq and ChIP-Seq analysis in order to reveal a conserved set of targets that explain the role of PAX8 in HGSC [31,32]. Further, because PAX8 is a lineage specific factor required for development of the urogenital system, the oncogenic roles of the protein appear to be acquired and unique in fallopian tube derived cancers. When looking at genetic variation associated with HGSC, genes that are targeted by PAX8 are enriched [41]. In fact, genome wide studies indicate that PAX8 also acts outside of promoter regions and can function more often to regulate gene expression by binding enhancers [32]. Epigenetics also reprograms the binding sites for PAX8 and offers expanded target genes when comparing RNA-Seq data in immortalized fallopian tube secretory cell lines and high grade serous cancer cell lines [31]. Further, single cell sequencing analysis suggests that PAX8/OVGP1<sup>high</sup> fallopian tube cells can be separated further into 3 clusters based on expression of KRT7, ESR1, and WFDC2, which may play a role in the heterogeneity of cancers formed from these subtypes [42]. One mechanism for a diverse action of PAX8 in different cell lines is the recruitment of co-regulators of PAX8, whereby data shows key roles for proteins such as TEAD1 and TEAD3 [32]. Another important PAX8 co-regulator is p53, which is positively regulated by PAX8 and shows differential expression and function on being mutated [26]. Despite all of these sequencing datasets, few studies have focused on PAX8 proteome and secretome, which would be targeted by a small molecule, provide a mechanism for cell death, and potentially serve as a therapeutic biomarker in HGSC. Additionally, this study provides another layer for interrogating the regulation of the high grade serous TME and proteins regulated by PAX8 expression.

Fibronectin is one of the major components of ECM and is used as a prognostic marker in ovarian cancer [7]. Fibronectin promotes cell invasion and migration via regulation of FAK-PI3K/Akt pathway and is secreted by human mesothelial cells to promote metastasis in ovarian cancer [8,9]. In 3D cultures, increased fibronectin expression promotes secondary metastasis by enhancing attachment of cancer cells to secondary organs [43]. Additionally, fibronectin has PAX8 binding sites upstream of the transcription start site [31]. So far, RNA-Seq and ChIP-Seq datasets examining targets of PAX8 indicate fibronectin as a direct target of PAX8 [31,32]. This explains our data that PAX8 loss reduces fibronectin expression causing loss of 3D spheroid integrity and reduced cell invasion and confirms at the protein level that PAX8 regulates ECM production by epithelial tumor cells.

Due to the ubiquitous nature of PAX8 expression in HGSC, regardless of cell origin, and the association of its reduced expression with decreasing tumor burden, a PAX8 inhibitor would be a promising drug target against various types of HGSC. Thus, identifying novel inhibitors of PAX8 expression may impact multiple aspects of ovarian cancer physiology and tumors derived from both OSE and FTE. Previously, we identified thioestron as an inhibitor of PAX8 expression [16]. Although thioestron significantly reduced tumor burden in ovarian cancer, it is not a viable drug lead due to toxicity and poor solubility, which we could overcome only with micelle-based delivery strategies [16]. Hence, we developed a PAX8 promoter-based screening assay and screened the Prestwick library of compounds. These compounds are FDA approved which potentially expedites clinical trials and facilitates therapeutic potential. Primary and secondary screening assays identified losartan and captopril as novel inhibitors of PAX8 promoter and protein expression. These hits significantly reduced expression PAX8 downstream targets such as FOXM1 and PKC $\alpha$  and reduced fibronectin expression in 2D and 3D cell models. In a matrigel invasion assay, both losartan and captopril caused significant reduction in cell invasion similar to loss of PAX8 expression. Losartan and captopril did not reduce viability of 3D tumor spheroids unlike thioestron which significantly reduced spheroid via-

bility at higher concentration. This may be due in part to higher reduction in PAX8 expression by thioestron wherein it triggers apoptosis, while losartan and captopril resulted in less repression of PAX8 expression and could therefore only influence the invasion phenotype.

Losartan and captopril are angiotensin-converting enzyme (ACE) inhibitors and used clinically to lower blood pressure [36,44]. Losartan has anti-fibrotic activity leading to dose-dependent reduction in stromal collagen and improves efficacy of nanotherapeutics in tumors [35]. In ovarian tumors, losartan caused a reduction in tumor ECM, decreased ascites and improved response to chemotherapy, which based on our results may be downstream of PAX8 [34]. Captopril is widely administered to manage congestive heart failure and also demonstrated anti-angiogenic activity in rat cornea [37,45]. This is interesting because PAX8 interacts with SOX17 transcription factor to regulates tumor angiogenesis in ovarian cancer [46]. Our data strongly suggests a role of PAX8 in modulating ECM making both losartan and captopril interesting drug leads in HGSC.

Future studies will focus on understanding how losartan and captopril regulate PAX8 expression and test these compounds *in vivo* to study their effect on HGSC tumor growth and ECM deposition. It would be interesting to know if these compounds regulate interaction of PAX8 with its co-regulators such as p53, SOX17, MECOM or TEAD and drive ovarian cancer progression. Previous studies have identified histone deacetylase (HDAC) inhibitors and CDK12/13 inhibitors to downregulate PAX8 expression leading to tumor reduction [39,47]. In this study, we identified losartan and captopril as novel PAX8 inhibitors and demonstrated that these inhibitors regulate PAX8 mediated secretion of fibronectin, cell invasion and tumor spheroid integrity.

#### Financial Support

DOD CDMRP OC 160076 Ovarian Cancer Pilot  
DOD CDMRP OC 210095 Teal Expansion

#### Data availability statement

The datasets generated during and/or analyzed during the current study are available from the corresponding author on reasonable request.

#### Conflict of interest statement

The authors declare that they have no known competing financial interests or personal relationships that could have appeared to influence the work reported in this paper.

#### CRediT authorship contribution statement

**Amrita Salvi:** Conceptualization, Data curation, Formal analysis, Investigation, Methodology, Validation, Visualization, Writing – original draft, Writing – review & editing. **Laura R. Hardy:** Conceptualization, Data curation, Formal analysis, Investigation, Methodology, Validation, Visualization, Writing – review & editing. **Kimberly N. Heath:** Data curation, Investigation, Methodology, Validation, Visualization, Writing – review & editing. **Samantha Watry:** Data curation, Investigation, Methodology, Validation, Visualization. **Melissa R. Pergande:** Data curation, Formal analysis, Investigation, Methodology, Validation, Visualization. **Stephanie M. Cologna:** Data curation, Formal analysis, Investigation, Methodology, Validation, Visualization, Writing – review & editing. **Joanna E. Burdette:** Conceptualization, Data curation, Formal analysis, Funding acquisition, Investigation, Methodology, Supervision, Validation, Visualization, Writing – original draft, Writing – review & editing.

## References

- [1] K. Wright, PARP inhibitors as frontline treatment in patients with ovarian cancer, *Oncology* (Williston Park, NY) 34 (3) (2020) Mar 19.
- [2] GM Rodriguez, KJC Galpin, CW McCloskey, BC. Vanderhyden, The tumor microenvironment of epithelial ovarian cancer and its influence on response to immunotherapy, *Cancers* 10 (8) (2018) 242 Aug.
- [3] NA Bhowmick, A Chytil, D Plieth, AE Gorska, N Dumont, S Shappell, et al., TGF- $\beta$  signaling in fibroblasts modulates the oncogenic potential of adjacent epithelia, *Science* 303 (5659) (2004) 848–851 Feb 6.
- [4] E Sahai, I Atsaturuv, E Cukierman, DG DeNardo, M Egeblad, RM Evans, et al., A framework for advancing our understanding of cancer-associated fibroblasts, *Nat. Rev. Cancer* 20 (3) (2020) 174–186 Mar.
- [5] DJ Cheon, Y Tong, MS Sim, J Dering, D Berel, X Cui, et al., A collagen-remodeling gene signature regulated by TGF $\beta$  signaling is associated with metastasis and poor survival in serous ovarian cancer, *Clin. Cancer Res.* 20 (3) (2014) 711–723 Feb 1.
- [6] G Efthymiou, A Saint, M Ruff, Z Rekad, D Ciais, E. Van Obberghen-Schilling, Shaping up the tumor microenvironment with cellular fibronectin, *Front. Oncol* 10 (2020) 66–83 Apr 30.
- [7] KA Kujawa, E Zembala-Nożyńska, AJ Cortez, T Kujawa, J Kupryjańczyk, KM. Lisowska, Fibronectin and periostin as prognostic markers in ovarian cancer, *Cells* 9 (1) (2020) 149 Jan 8.
- [8] NG. Yousif, Fibronectin promotes migration and invasion of ovarian cancer cells through up-regulation of FAK–PI3K/Akt pathway, *Cell Biol. Int.* 38 (1) (2014) 85–91.
- [9] HA Kenny, CY Chiang, EA White, EM Schryver, M Habis, IL Romero, et al., Mesothelial cells promote early ovarian cancer metastasis through fibronectin secretion, *J. Clin. Investig.* 124 (10) (2014) 4614–4628 Oct 1.
- [10] A Yokoi, T Matsumoto, Y Oguri, Y Hasegawa, M Tochimoto, M Nakagawa, et al., Upregulation of fibronectin following loss of p53 function is a poor prognostic factor in ovarian carcinoma with a unique immunophenotype, *Cell Commun. Signal.* 18 (1) (2020) 103 Jul 7.
- [11] YL Huang, CY Liang, D Ritz, R Coelho, D Septiadi, M Estermann, et al., Collagen-rich omentum is a premetastatic niche for integrin  $\alpha$ 2-mediated peritoneal metastasis, *Elife* 9 (2020) e59442 Oct 7.
- [12] R. Kurman, Origin and molecular pathogenesis of ovarian high-grade serous carcinoma, *Ann. Oncol.* 24 (suppl 10) (2013) x16–x21.
- [13] JA Blake, MR. Ziman, Pax genes: regulators of lineage specification and progenitor cell maintenance, *Development* 141 (4) (2014) 737–751 Feb 15.
- [14] AR Laury, JL Hornick, R Perets, JF Krane, J Corson, R Drapkin, et al., PAX8 reliably distinguishes ovarian serous tumors from malignant mesothelioma, *Am. J. Surg. Pathol.* 34 (5) (2010) 627–635 May.
- [15] E Adler, P Mhawech-Fauceglia, SA Gayther, K. Lawrenson, PAX8 expression in ovarian surface epithelial cells, *Hum. Pathol.* 46 (7) (2015) 948–956 Jul.
- [16] LR Hardy, MR Pergande, K Esparza, KN Heath, H Önyüksel, SM Cologna, et al., Proteomic analysis reveals a role for PAX8 in peritoneal colonization of high grade serous ovarian cancer that can be targeted with micelle encapsulated thiostrepton, *Oncogene* 1 (2019) 6003–6016 Jul 11.
- [17] NJ Bowen, S Logani, EB Dickerson, LB Kapa, M Akhtar, BB Benigno, et al., Emerging roles for PAX8 in ovarian cancer and endosalpingeal development, *Gynecol. Oncol.* 104 (2) (2007) 331–337 Feb.
- [18] LR Hardy, A Salvi, JE. Burdette, UnPAXing the divergent roles of PAX2 and PAX8 in high-grade serous ovarian cancer, *Cancers* 10 (8) (2018) 262 Aug.
- [19] LH Rodgers, Loss of PAX8 in high-grade serous ovarian cancer reduces cell survival despite unique modes of action in the fallopian tube and ovarian surface epithelium, *OncoTargets Ther.* 7 (2) (2016) 32785–32795 May 31.
- [20] AS Nagaraja, RL Dood, G Armaiz-Pena, Y Kang, SY Wu, JK Allen, et al., Adrenergic-mediated increases in INHBA drive CAF phenotype and collagens, *JCI Insight* 6 (7) (2021) e149895 May 19.
- [21] SE Ong, M. Mann, A practical recipe for stable isotope labeling by amino acids in cell culture (SILAC), *Nat. Protoc.* 1 (6) (2006) 2650–2660 Dec.
- [22] JR Wiśniewski, A Zougman, N Nagaraj, M. Mann, Universal sample preparation method for proteome analysis, *Nat. Methods* 6 (5) (2009) 359–362 May.
- [23] A Salvi, CSM Amrine, JR Austin, K Kilpatrick, A Russo, D Lantvit, et al., Verticillin A causes apoptosis and reduces tumor burden in high-grade serous ovarian cancer by inducing DNA damage, *Mol. Cancer Ther.* 19 (1) (2020) 89–100 Jan 1.
- [24] SM King, TS Hilliard, LY Wu, RC Jaffe, AT Fazleabas, JE. Burdette, The impact of ovulation on fallopian tube epithelial cells: evaluating three hypotheses connecting ovulation and serous ovarian cancer, *Endocr. Relat. Cancer* 18 (5) (2011) 627–642 Oct.
- [25] AA Soriano, T de Cristofaro, T Di Palma, S Dotolo, P Gokulnath, A Izzo, et al., PAX8 expression in high-grade serous ovarian cancer positively regulates attachment to ECM via Integrin  $\beta$ 3, *Cancer Cell Int.* 19 (1) (2019) 303 Nov 20.
- [26] D Ghannam-Shahbari, E Jacob, RR Kakun, T Wasserman, L Korsensky, O Sternfeld, et al., PAX8 activates a p53-p21-dependent pro-proliferative effect in high grade serous ovarian carcinoma, *Oncogene* 37 (17) (2018) 1–12 Jan 23.
- [27] T Di Palma, V Lucci, T de Cristofaro, MG Filippone, M. Zannini, A role for PAX8 in the tumorigenic phenotype of ovarian cancer cells, *BMC Cancer* 14 (2014) 292 Apr 26.
- [28] Cristofaro T de, Palma TD, AA Soriano, A Monticelli, O Affinito, S Coccozza, et al., Candidate genes and pathways downstream of PAX8 involved in ovarian high-grade serous carcinoma, *OncoTargets Ther.* 7 (27) (2016) 41929–41947 May 31.
- [29] M Bleu, F Mermet-Meillon, V Apfel, L Barys, L Holzer, Bachmann Salvy M, et al. PAX8 and MECOM are interaction partners driving ovarian cancer, *Nat. Commun.* 12 (1) (2021) 2442 Apr 26.
- [30] ME Katt, AL Placone, AD Wong, ZS Xu, PC. Seanson, In Vitro tumor models: advantages, disadvantages, variables, and selecting the right platform, *Front. Bioeng. Biotechnol.* 4 (12) (2016) Feb 12.
- [31] KM Elias, MM Emori, T Westerling, H Long, A Budina-Kolomets, F Li, et al., Epigenetic remodeling regulates transcriptional changes between ovarian cancer and benign precursors, *JCI Insight* 1 (13) (2016) e87988 Aug 18.
- [32] EK Adler, RI Corona, JM Lee, N Rodriguez-Malave, P Mhawech-Fauceglia, H Sowter, et al., The PAX8 cistrome in epithelial ovarian cancer, *OncoTargets Ther.* 8 (2017) 108316–108332 Dec 12.
- [33] A di Gennaro, O Spadaro, MG Baratta, M De Felice, R. Di Lauro, Functional analysis of the murine Pax8 promoter reveals autoregulation and the presence of a novel thyroid-specific DNA-binding activity, *Thyroid* 23 (4) (2013) 488–496 Apr.
- [34] Y Zhao, J Cao, A Melamed, M Worley, A Gockley, D Jones, et al., Losartan treatment enhances chemotherapy efficacy and reduces ascites in ovarian cancer models by normalizing the tumor stroma, *Proc. Natl. Acad. Sci.* 116 (6) (2019) 2210–2219 Feb 5.
- [35] B Diop-Frimpong, VP Chauhan, S Krane, Y Boucher, RK. Jain, Losartan Inhibits Collagen I Synthesis and Improves the Distribution and Efficacy of Nanotherapeutics in Tumors, *PNAS* 108 (7) (2011) 2909–2914 Feb 15.
- [36] PK Siegl, SD Kivlighn, TP. Broten, Pharmacology of losartan, an angiotensin II receptor antagonist, in animal models of hypertension, *J. Hypertens. Suppl.* 13 (1) (1995) S15–S21 Jul.
- [37] OV Volpert, WF Ward, MW Linggen, L Chesler, DB Solt, MD Johnson, et al., Captopril inhibits angiogenesis and slows the growth of experimental tumors in rats, *J. Clin. Investig.* 98 (3) (1996) 671–679 Aug 1.
- [38] T. Gamberi, Proteomic analysis of PAX8 alterations provides new insights into its role as a master regulator of migration in high-grade serous ovarian cancer, *Ann. Transl. Med.* 7 (Suppl 8) (2019) S303 Dec.
- [39] K Shi, X Yin, MC Cai, Y Yan, C Jia, P Ma, et al., PAX8 regulon in human ovarian cancer links lineage dependency with epigenetic vulnerability to HDAC inhibitors, *eLife* 8 (2019) e44306 May 3.
- [40] OMT Pearce, RM Delaine-Smith, E Maniati, S Nichols, J Wang, S Böhm, et al., Deconstruction of a metastatic tumor microenvironment reveals a common matrix response in human cancers, *Cancer Discov.* 8 (3) (2018) 304–319, Dec 1.
- [41] SP Kar, E Adler, J Tyrer, D Hazelett, H Anton-Culver, EV Bandera, et al., Enrichment of Putative PAX8 Target Genes at Serous Epithelial Ovarian Cancer Susceptibility Loci, *British Journal of Cancer* 116 (2017) 524–535 Jan 19.
- [42] HQ Dinh, X Lin, F Abbasi, R Nameki, M Haro, CE Olingy, et al., Single-cell transcriptomics identifies gene expression networks driving differentiation and tumorigenesis in the human fallopian tube, *Cell Rep.* 35 (2) (2021) 108978 Apr 13.
- [43] HJ Park, DM. Helfman, Up-regulated fibronectin in 3D culture facilitates spreading of triple negative breast cancer cells on 2D through integrin  $\beta$ -5 and Src, *Sci. Rep.* 9 (1) (2019) 19950 Dec 27.
- [44] BH Migdalof, MJ Antonaccio, Mc Kinstry DN, SM Singhvi, SJ Lan, P Egli, et al., Captopril: pharmacology, metabolism, and disposition, *Drug Metab. Rev.* 15 (4) (1984) 841–869 Jan 1.
- [45] MA Pfeffer, E Braunwald, LA Moyé, L Basta, EJ Brown, TE Cuddy, et al., Effect of captopril on mortality and morbidity in patients with left ventricular dysfunction after myocardial infarction, *N. Engl. J. Med.* 327 (10) (1992) 669–677 Sep 3.
- [46] Chaves-Moreira D, Mitchell MA, Arruza C, Rawat P, Sidoli S, Nameki R, et al. PAX8 orchestrates an angiogenic program through interaction with SOX17 [Internet]. *bioRxiv*; 2020 [cited 2022 Jan 21]. p. 2020.09.09.290387. Available from: <https://www.biorxiv.org/content/10.1101/2020.09.09.290387v1>.
- [47] L Lin, K Shi, S Zhou, MC Cai, C Zhang, Y Sun, et al., SOX17 and PAX8 constitute an actionable lineage-survival transcriptional complex in ovarian cancer, *Oncogene* 41 (12) (2022) 1767–1779 Mar.